

# Major Histocompatibility Complex (MHC) Class II–Positive Dendritic Cells in the Rat Iris

## In Situ Development From MHC Class II–Negative Precursors

Raymond J. Steptoe,\*† Patrick G. Holt,\* and Paul G. McMenemy†

**Purpose.** To examine the postnatal development of major histocompatibility complex (MHC) class II–positive dendritic cells (DC) in the iris of the normal rat eye.

**Methods.** Single- and double-color immunomorphologic studies were performed on whole mounts prepared from rat iris taken at selected postnatal ages (2 to 3 days to 78 weeks). Immunopositive cells were enumerated, using a quantitative light microscope, and MHC class II expression on individual cells was assessed by microdensitometric analysis.

**Results.** Major histocompatibility class II–positive DCs in the iris developed in an age-dependent manner and reached adult-equivalent density and structure at approximately 10 weeks of age, considerably later than previously described in other DC populations in the rat. In contrast, the anti-rat DC monoclonal antibody OX62 revealed a population of cells present at adult-equivalent levels as early as 3 weeks after birth. Dual-color immunostaining and microdensitometric analysis demonstrated that during postnatal growth, development of the network of MHC class II–positive DCs was a consequence of the progressive increase in expression of MHC class II antigen by OX62-positive cells.

**Conclusions.** During postnatal growth, the DC population of the iris develops initially as an OX62-positive–MHC class II–negative population, which then develops increasing MHC class II expression in situ and finally resembles classic DC populations in other tissue sites. Maturation of the iris DC population is temporally delayed compared with time to maturation in other tissue sites in the rat. *Invest Ophthalmol Vis Sci.* 1997;38:2639–2648.

In recent studies, the presence of separate and distinct networks of resident tissue macrophages and major histocompatibility complex (MHC) class II (Ia)–positive dendritic cells (DCs) in tissues bordering the anterior chamber (AC) of a range of species has been described.<sup>1–3</sup> This population of DCs accounts for virtually all Ia immunostaining in the iris and is present at densities similar to that of Ia<sup>+</sup> epidermal Langerhans' cells.<sup>3</sup> These features, combined with the evidence that rat iris Ia<sup>+</sup> DCs possess a potent ability to stimulate primary immune responses in vitro,<sup>4</sup> sug-

gests that these cells may play an important role in immune surveillance of the anterior chamber.

The ontogeny of Ia<sup>+</sup> DC populations during fetal and postnatal development has been examined in a number of lymphoid and nonlymphoid tissues. In the rat, Ia<sup>+</sup> DC populations are first observed at fetal day 15 in the thymus and subepithelial tissues of the gastrointestinal tract as collections of rounded or macrophage-like Ia<sup>low</sup> cells,<sup>5–7</sup> which then increase in numbers and upregulate Ia expression during fetal development.<sup>8,9</sup> After birth, DC populations in the rat attain adult-equivalent levels within 2 to 3 weeks in virtually all tissue sites examined to date.<sup>5,6,8,10–13</sup>

Reports of results from previous qualitative studies on frozen sections from this laboratory have suggested that the development of Ia<sup>+</sup> DCs in the aqueous outflow pathways of the rat eye may occur more slowly than that observed in other tissue sites.<sup>14</sup> Therefore, we sought to evaluate the postnatal development of Ia<sup>+</sup> DCs in the anterior uveal tract, using a whole

From the \*TVW Telethon Institute for Child Health Research, Subiaco, Western Australia; †and the Department of Anatomy and Human Biology, The University of Western Australia, Nedlands, Perth, Western Australia.

Supported in part by the National Health and Medical Research Council (NH and MRC). RJS received an Australian Postgraduate Research Award.

Submitted for publication; revised; accepted.

Proprietary interest category: N.

Reprint requests: Paul G. McMenemy, Department of Anatomy and Human Biology, The University of Western Australia, Nedlands, 6907 Western Australia, Australia.

mount technique to allow visualization of the entire DC population within this tissue. Evidence presented in this report indicates that DCs infiltrate the iris primordium as Ia<sup>negative</sup> or Ia<sup>low</sup> precursor cells, which subsequently develop in situ into DC-bearing high levels of Ia antigen. Furthermore, the data of the present study indicate that although Ia<sup>+</sup> DC development in the iris may be morphologically similar to that in other tissue sites, this process is delayed temporally and occurs at a considerably slower rate than that reported in many other tissue sites of the rat.

## MATERIALS AND METHODS

### Animals

Male Lewis rats (specific pathogen free) were purchased from the Animal Resources Centre (Murdoch, Australia). Seventy-three eyes from 52 animals were used. Animals were housed in the animal research center at Princess Margaret Hospital (Subiaco, WA, Australia) under National Health and Medical Research Council-approved conditions. All procedures conformed to the ARVO Statement for the Use of Animals in Ophthalmic and Vision Research.

### Monoclonal Antibodies

The monoclonal antibody (mAb) OX6 (anti-Ia),<sup>15</sup> OX8 (anti-CD8),<sup>16</sup> OX19 (anti-CD5),<sup>17</sup> OX21 (anti-human iC3b; isotype control),<sup>18</sup> OX22 (anti-CD45RC)<sup>19</sup> and OX62 (anti-DC, veiled cells, and  $\gamma\delta$ TCR<sup>+</sup> T cells)<sup>20</sup> were kindly supplied by Dr. D. Mason (Dunn School of Pathology, Oxford, UK). ED2 (anti-resident tissue macrophage)<sup>21</sup> was provided by Dr. C. Dijkstra (Vrije University, Amsterdam, The Netherlands). Dr. T. Hunig (University of Wurzburg, Germany) kindly provided the mAb R73 (anti- $\alpha\beta$ TCR)<sup>22</sup> and V65 (anti- $\gamma\delta$ TCR).<sup>23</sup> Other mAbs used have been previously reported: RP3 (antipolymorphonuclear neutrophil),<sup>24</sup> G4.18 (anti-CD3),<sup>25</sup> and HIS-14 (anti-B cell).<sup>26,27</sup> Biotinylated mAbs were generated in-house at TVW Telethon Institute for Child Health Research. Streptavidin-horseradish peroxidase (S-HRP), biotinylated sheep anti-mouse immunoglobulin (Ig) G (biotin-SHAM), sheep anti-mouse IgG-horseradish peroxidase conjugate and streptavidin-alkaline phosphatase conjugates were purchased from Amersham (Sydney, Australia).

### Immunohistochemical Staining

Irises from cardiac-perfused animals (phosphate-buffered saline plus heparin) were prepared for whole mount immunostaining, as previously described,<sup>3,28</sup> or were prepared for cryostat sectioning by infiltration with embedding medium (OCT; Tissue-Tek, Elkhart, CA) and freezing, as previously described.<sup>14</sup> Whole-

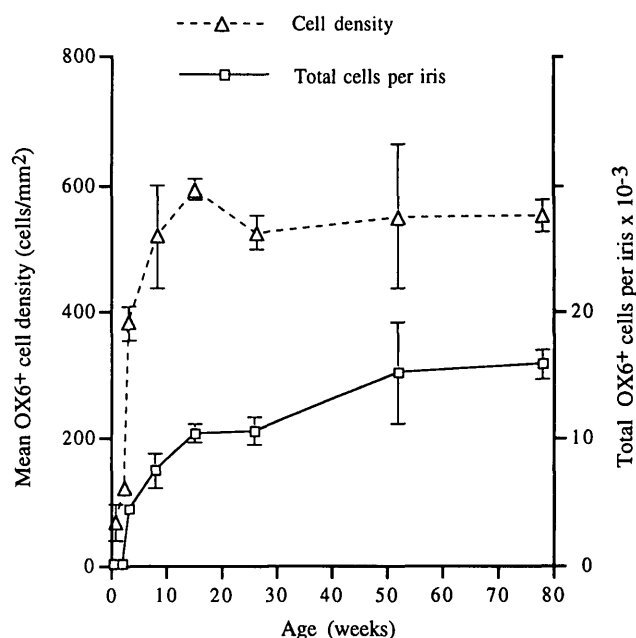


**FIGURE 1.** Development of major histocompatibility complex class II (OX6)<sup>+</sup> iris dendritic cells during postnatal growth. Data are mean  $\pm$  SD compiled from eight eyes (four animals) of 2- to 3-day-old animals and in five to six eyes (three animals) of other groups.

ounts to be stained with OX62 were postfixed in cold ethanol (5 minutes) before rehydration in phosphate-buffered saline. Frozen sections (10  $\mu$ m) were cut, placed on gelatinized slides and air dried (30 minutes) before rehydration and immunostaining. Single-color immunohistochemical staining and double-color immunohistochemical staining were performed as previously described.<sup>3,10</sup>

For microdensitometric analysis, Ia<sup>+</sup> cells were stained immunohistochemically with the mAb OX6 and subsequent incubations with biotin-SHAM and S-HRP. The enzyme substrate development step (using 3,3 diaminobenzidine tetrahydrochloride; Sigma, St. Louis, MO) was terminated before generation of saturating concentrations of substrate reaction product. Results of preliminary experiments (data not shown) revealed that although prolonged incubation resulted in staining of greater intensity, the differential staining intensity between individual DCs was obscured.

### Quantitative Analysis

Enumeration of immunopositive cells in iris wholemounts was performed as previously described.<sup>3</sup> Assessment of the morphologic characteristics of iris DCs in wholemounts was performed by classification of immunopositive cells as round, pleomorphic, or dendriform during enumeration. Cells classified as round comprised small, round cells up to 12  $\mu$ m in diameter, which displayed no evidence of surface projections or cell processes. Pleomorphic cells included regular-

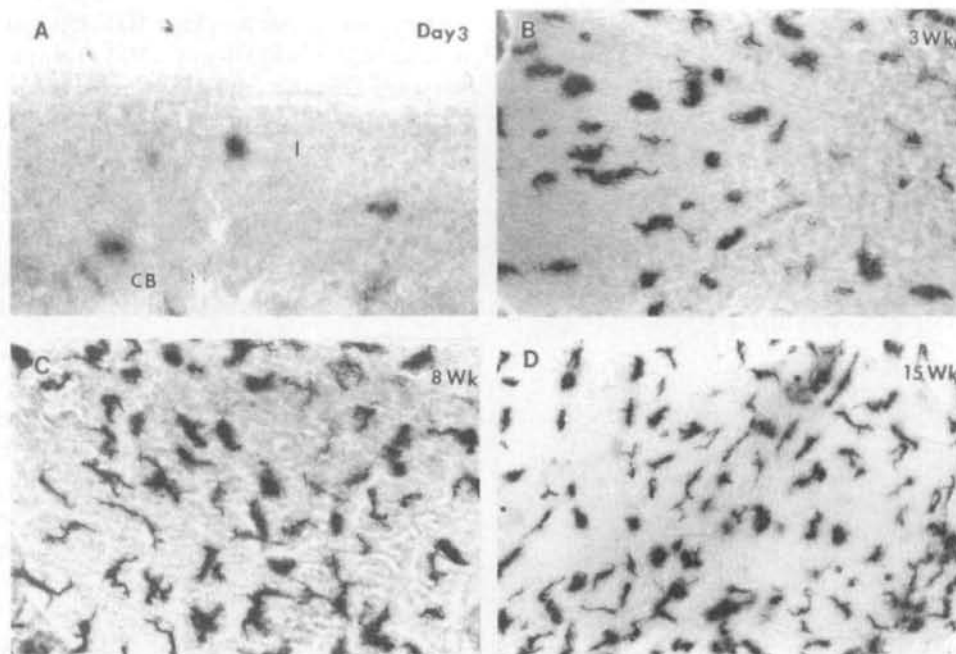


**FIGURE 2.** Immunomorphologic illustration of major histocompatibility complex class II (OX6)<sup>+</sup> iris dendritic cell development during postnatal growth in rat iris wholemounts. (A) A 3-day-old animal: The developing iris (I) is visible as a thin band of tissue. The ciliary body (CB) is poorly differentiated at this stage. Note the relatively low number of immunopositive cells in these newborn rats. (B) Three-week-old animals: Cells are predominantly pleomorphic, although unipolar and bipolar cells are common. Some cells exhibit a veiled appearance evident at higher magnification (not shown). (C) An 8-week-old animal: Cell density is similar to older animals, but the cells are not as highly dendriform as in older animals. (D) A 15-week-old animal: Cells exhibit extensive cell processes and high MHC class II (Ia) antigen expression. Magnifications: (A, B)  $\times 250$ .

shaped cells larger than  $12 \mu\text{m}$  in diameter and those that demonstrated evidence of some surface projections (veils, ruffles) or cells displaying a unipolar or bipolar structure whose cell processes were broad, short, and unbranched. Cells were classified as dendriform cells when they possessed more than two cell processes projecting from the cell body or when they displayed one or two long, fine, branched cell processes. The proportion of cells in each morphologic category was expressed as a percentage of the total number of cells.

The surface area of the irides was determined microscopically, using image analysis software (OPTIMAS 4.0, Bioscan, Edmonds, WA). Only whole irides were used to determine area. Total number of immunopositive cells per iris was calculated for each individual iris wholemount by multiplication of the mean cell densities and total iris areas.

Microdensitometry of individual cells was performed using computerized image analysis (Chromatic Image Analysis System MD-30, Flinders Imaging, Adelaide, Australia), as previously described.<sup>10</sup> Staining conditions were rigorously standardized between individual immunostaining sessions, each of which included internal (adult) controls. To minimize interex-

perimental variation, the number of staining runs required to obtain all age groups was limited to three. When performing microdensitometry on different developmental age groups, between 25 and 45 cells were analyzed per iris (mean, 35.4), resulting in analysis of between 199 and 315 cells per age group.

### Statistical Analysis

Percentage values were arcsine transformed to adjust for nonnormality before statistical analysis.<sup>29</sup> Regression analysis of Ia expression with age was performed.

## RESULTS

### Postnatal Development of Major Histocompatibility Complex Class II-Positive Iris Dendritic Cells

Previous immunomorphologic studies of adult rats<sup>3,4</sup> have demonstrated the presence of a network of pleomorphic and dendriform Ia<sup>+</sup> iris DCs present in Lewis rats at a density of approximately 450 cells/mm<sup>2</sup>. Quantitative analysis of anti-Ia-immunostained iris wholemounts revealed that the Ia<sup>+</sup> iris DC population of the Lewis rat increased in density during postnatal

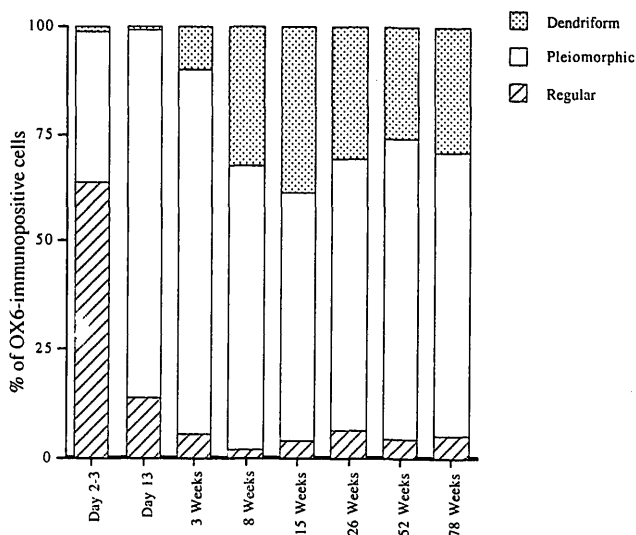


**FIGURE 3.** Quantitative analysis of the structure of major histocompatibility complex class II (OX6)<sup>+</sup> iris dendritic cells during postnatal development. Data were compiled using a quantitative microscope as detailed in Materials and Methods and comprise identical group sizes, as presented in Figure 1.

development and attained adult equivalent density approximately 8 to 10 weeks after birth (Fig. 1). It is notable that the density of Ia<sup>+</sup> cells was maximum at 15 weeks of age. After a small reduction, Ia<sup>+</sup> cell density was maintained at a relatively stable level throughout adulthood. The total number of Ia<sup>+</sup> cells present in each iris followed a similar pattern of postnatal development and attained a value throughout adulthood (approximately 11,000 to 15,000 cells/iris) that reflected total iris area (Fig. 1).

Qualitative and quantitative examination revealed that in 2- to 3-day-old neonates, anti-Ia immunostaining delineated a cell population comprised predominantly of small (12 to 15  $\mu\text{m}$  in diameter), rounded cells (Fig. 2A), although unipolar or bipolar (pleiomorphic) cells were noted (Fig. 3). The iris at this age is only approximately 200 to 300  $\mu\text{m}$  in width. By postnatal day 13, a larger proportion (more than 80%) of Ia<sup>+</sup> cells exhibited a greater degree of pleiomorphic structure. Many cells exhibited a "veiled" appearance, and unipolar or bipolar cells were not uncommon; however, dendriform cells were rarely observed (Fig. 3). Cells that exhibited pleiomorphic structure comprised the greatest proportion of immunopositive cells in 3-week-old Lewis rat irises (Fig. 2B). Although dendriform cells were present, they constituted a small proportion of the population (Fig. 3). By 8 weeks of age, Ia<sup>+</sup> cells exhibited cell density and morphologic characteristics similar to those of adult animals (Fig. 2C), but the extent of dendrite expression by Ia<sup>+</sup> cells appeared somewhat less evident than that observed in

15-week-old animals (Fig. 2D). Quantitative examination of the intensity of anti-Ia immunoperoxidase staining (Fig. 4) revealed that Ia expression exhibited a gradual increase during postnatal growth and reached a value closely approximating that observed throughout maturity by 8 weeks after birth ( $r = 0.855$ ).

### Delineation of Iris Dendritic Cell Development With the Monoclonal Antibody OX62

The mAb OX62, which was raised against rat veiled cells, recognizes a surface marker on rat DCs in lymphoid and nonlymphoid tissues and  $\gamma\delta$  TCR<sup>+</sup> T cells in the epidermis (putative dendritic epidermal T cells).<sup>20</sup> Examination of rat iris wholemounts with the mAb OX62 revealed that in 2- to 3-day-old neonatal animals, immunopositive cells were present at a density ( $240 \pm 85$  cells/ $\text{mm}^2$ ) approximately four times that observed in Ia<sup>+</sup> cells ( $66.5 \pm 28.2$  cells/ $\text{mm}^2$ ; Fig. 5A). Immunopositive cells were predominantly small (10 to 12  $\mu\text{m}$  in diameter) and exhibited a rounded structure with highly indented or cleft nuclei; however, a small number of cells were slightly larger (12 to 15  $\mu\text{m}$  diameter) and exhibited a finely ruffled cell surface, visible by high-power magnification. Cells that exhibited a unipolar structure were also rarely observed. At postnatal day 13,

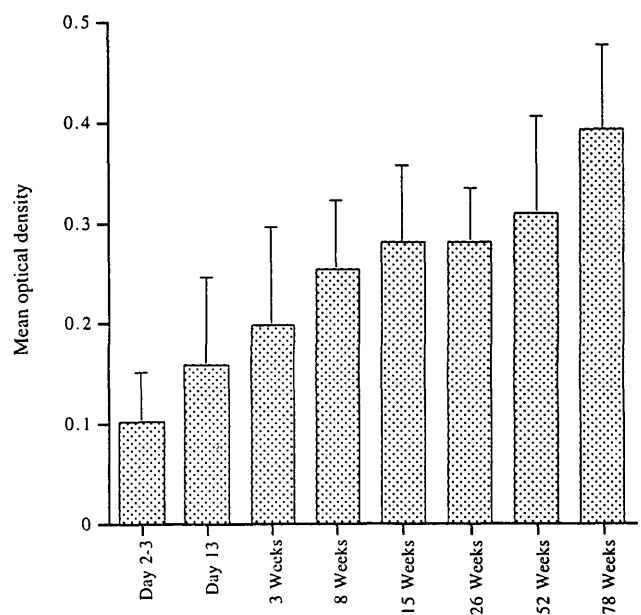


**FIGURE 4.** Anti-major histocompatibility complex class II (OX6) immunoperoxidase staining intensity of iris dendritic cells during postnatal development. Major histocompatibility class II (Ia) staining intensity was determined with a microdensitometric technique in individual immunopositive cells and is presented as mean  $\pm$  SD. Optical density data were compiled from the same material analyzed for determination of cell density in Figure 1.

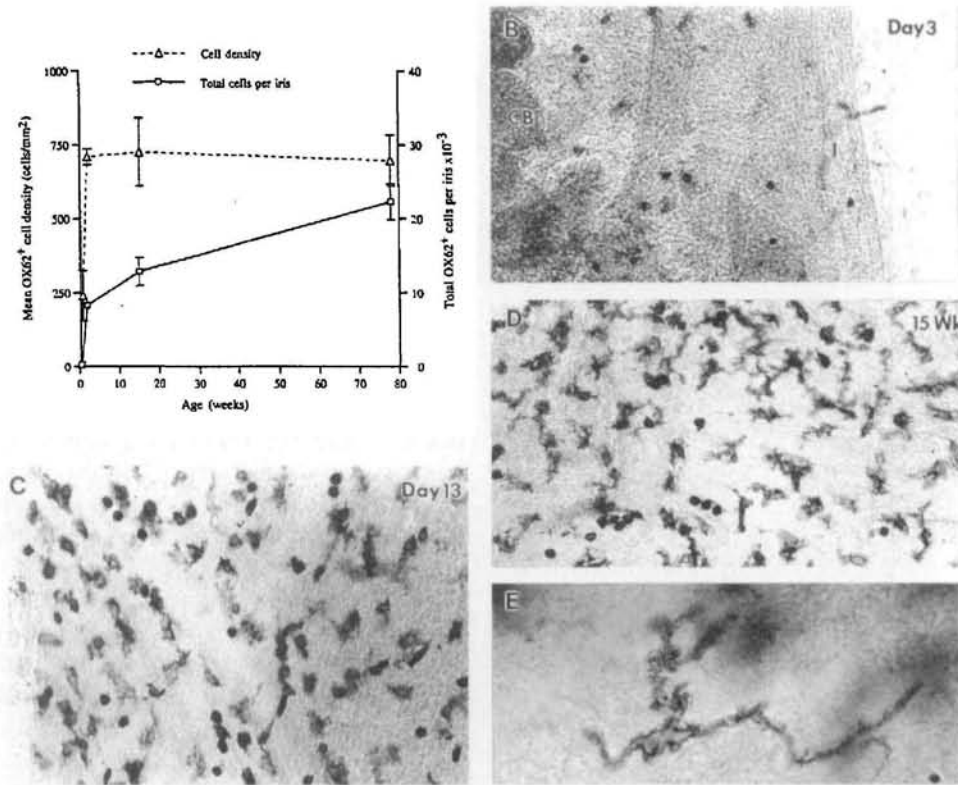


**FIGURE 5.** (A) Development of OX62<sup>+</sup> cells in the iris during postnatal development. Data are mean  $\pm$  SD compiled from four eyes (four animals) of 2- to 3-day-old and 13-day-old animals, from three eyes (two animals) of 15-week-old animals, and from two eyes (two animals) of 78-week-old animals. The total number of cells are calculated from mean cell density and areas presented in Figure 1. (B, C, D, E) Iris wholemounts immunostained with the anti-dendritic cell monoclonal antibody OX62. (B) A 3-day-old rat iris and ciliary body (CB) wholemount. Immunopositive cells are predominantly small and rounded. (C) A 3-week-old animal. Note that immunopositive cells are present at close to adult-equivalent levels; however, they are considerably less dendriform, compared with those in (D) 15-week-old animals, in which some immunopositive cells (E) exhibit highly dendriform structure. Magnifications: (B, C, D)  $\times 250$ , (E)  $\times 630$ .

OX62<sup>+</sup> cells were present in the iris at a density that closely approached that observed in adult animals (Fig. 5A). Cell structure was generally rounded (12 to 15  $\mu\text{m}$  in diameter); however, the predominant proportion of the population exhibited a small degree of elongation or irregularity in cell profile and ruffled cell margins that were visualized at high magnification. By postnatal week 15, a large proportion of the OX62<sup>+</sup> cells exhibited a well-developed dendriform structure (Figs. 5D, 6), with processes that spanned 60 to 100  $\mu\text{m}$  (Fig. 5E). A minor population of small (10 to 12  $\mu\text{m}$  in diameter), rounded, intensely OX62<sup>+</sup> cells appeared to be marginated within iris blood vessels (Fig. 7E). Also present was a population of slightly larger (12 to 15  $\mu\text{m}$  in diameter) irregular cells that often possessed short cell processes. The density and morphologic characteristics of OX62<sup>+</sup> cells in 78-week-old animals was similar to those in young adults.

#### Development of Major Histocompatibility Complex Class II Expression by OX62-Positive Iris Dendritic Cells

The observation of an extensive population of OX62<sup>+</sup> cells in the absence of comparable Ia expression in the iris during early postnatal development suggested delayed development of Ia expression by recently recruited iris DCs. Therefore, we sought to determine the coexpression of Ia antigens on OX62<sup>+</sup> cells by dual-color immunostaining studies. In 2- to 3-day-old rats, detectable levels of Ia were expressed on only a relatively small proportion of OX62<sup>+</sup> cells (15%; Figs. 7A, 8), and this expression was restricted to the population of slightly larger (12 to 15  $\mu\text{m}$  in diameter) OX62<sup>+</sup> cells (Fig. 7A). In 13-day-old rats, the proportion of OX62<sup>+</sup> cells expressing Ia was marginally greater (20%) than that of newborns (Figs. 7B, 8), with Ia expression largely restricted to the pleomor-

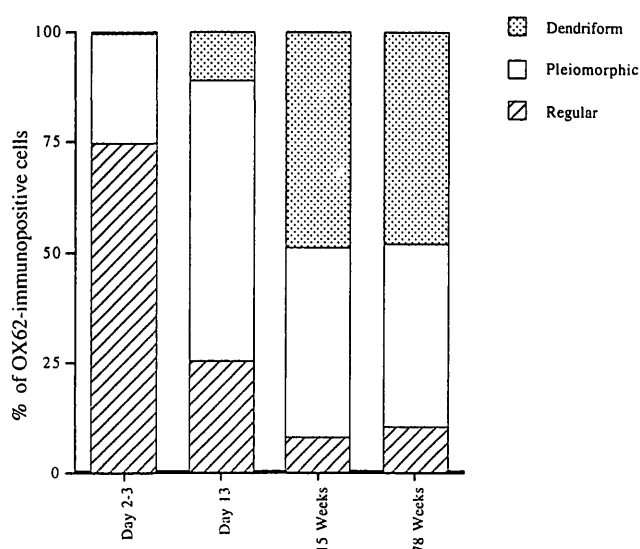


**FIGURE 6.** Quantitative analysis of OX62<sup>+</sup> iris dendritic cells during postnatal development. Data were compiled from four animals per group (3-day-old and 3-week-old) or two animals per group (5- and 78-week-old).

phic OX62<sup>+</sup> cells. The nuclear profile was invariably more irregular in double-immunopositive cells than that in the highly cleft nuclei observed in small, round OX62<sup>+</sup>/Ia<sup>-</sup> cells.

At 15 weeks, Ia was expressed on approximately two thirds of all OX62<sup>+</sup> cells (Figs. 7C, 8). The inner pupillary portion of the iris appeared to contain a slightly higher proportion of OX62<sup>+</sup>/Ia<sup>+</sup> cells, whereas many highly dendriform cells that spanned 40 to 60  $\mu\text{m}$  at the base of the iris were Ia<sup>-</sup>. In general, those OX62<sup>+</sup> cells that coexpressed Ia exhibited a more dendriform or pleiomorphic structure than those OX62<sup>+</sup>/Ia<sup>-</sup> cells. Small (10 to 12  $\mu\text{m}$  in diameter) OX62<sup>+</sup> cells were consistently Ia<sup>-</sup> (Fig. 7C, 7D); however, a large proportion of the rounded and slightly larger (12 to 15  $\mu\text{m}$  in diameter) "fuzzy" cells coexpressed Ia antigens (Fig. 7C). In an aged population of animals (18 months old), the proportion of OX62<sup>+</sup> cells coexpressing Ia was markedly higher than that observed in 15-week-old animals (Fig. 8). In these animals, Ia expression was restricted to pleiomorphic and dendriform cells.

Extensive immunostaining was performed that excluded the presence of significant numbers of CD3<sup>+</sup> (G4.18),  $\alpha\beta\text{TCR}^+$  (R73), or  $\gamma\delta\text{TCR}^+$  (V65) T lymphocytes, B cells (HIS-14) or polymorphonuclear neutrophils (RP3), consistent with results previously reported.<sup>28</sup> In addition, strong endogenous peroxidase activity, normally associated with eosinophils, was absent from negative-control wholemounts, suggesting these cells could also be excluded. Because Ia immunostaining within the iris was restricted virtually exclusively to OX62<sup>+</sup> cells (Fig. 8), it was therefore concluded that the small, round OX62<sup>+</sup>/Ia<sup>-</sup> cells com-

prised OX62<sup>+</sup>/Ia<sup>+</sup> DC precursors. Double-color immunostaining with the mAb OX62 and ED2 (resident-tissue, macrophage-specific mAb) excluded the possibility that OX62<sup>+</sup>/Ia<sup>-</sup> pleiomorphic and dendriform cells may have comprised macrophages.

## DISCUSSION

Previous immunomorphologic studies have delineated an Ia<sup>+</sup> DC network in the iris that resembles that seen in many other tissue sites.<sup>1,3</sup> Examination of the functional characteristics of Ia<sup>+</sup> cells enriched from the rat iris by positive immunomagnetic selection have demonstrated their potent capacity to induce primary immune responses in vitro, following maturational signals provided by granulocyte macrophage colony-stimulating factor,<sup>4</sup> indicating their potential as important mediators of immune surveillance in the anterior chamber, a classic site of immune privilege.<sup>30,31</sup> Results of previous qualitative studies from this laboratory have suggested that Ia<sup>+</sup> cell populations in tissues surrounding the AC and along the path of the aqueous outflow pathway in the rat may not attain adult-equivalent levels until after sexual maturity.<sup>14</sup> Such a pattern of development is in contrast with that reported in all other rat DC populations examined to date—for example, within the respiratory system,<sup>8,10</sup> gastrointestinal tract,<sup>5,6,11</sup> heart,<sup>12</sup> and pancreas.<sup>13</sup> The mAb OX62 has been used to delineate DC populations in a number of rat tissues, including spleen,<sup>20</sup> conducting airways,<sup>10</sup> small intestine,<sup>32</sup> and posterior uveal tract of the eye.<sup>33</sup> Use of this mAb for successful characterization of the development of rat DCs generated in vitro from bone marrow progenitor cells<sup>34</sup> and for demonstration of Ia<sup>-</sup> DC precursors in the conducting airways during postnatal development<sup>10</sup> indicate that this mAb, in conjunction with anti-Ia mAb, may be a valuable tool in investigations of DC development in the iris, allowing comparison with DC development in other tissue sites. The results of the current study suggest that Ia<sup>+</sup> DCs develop from OX62<sup>+</sup>/Ia<sup>-/low</sup> precursors. It should be noted, however, that OX62<sup>+</sup>/Ia<sup>-</sup> cells may have generally escaped detection in other tissues for technical reasons, in that we have found fixation and mode of tissue preparation to be crucial for successful immunostaining of OX62.

Single immunostaining with anti-Ia mAb revealed an age-dependent process of Ia<sup>+</sup> DC development in the iris that comprised transition from rounded cells with few cell processes that expressed relatively low levels of Ia through intermediate morphologic forms to the characteristic dendriform-pleiomorphic structure of DCs. These observations were similar to those reported on Ia<sup>+</sup> DCs in other tissue sites, leading previous workers to conclude that Ia<sup>+</sup> DCs develop in situ from Ia<sup>low</sup> cells observed in the early stages of DC

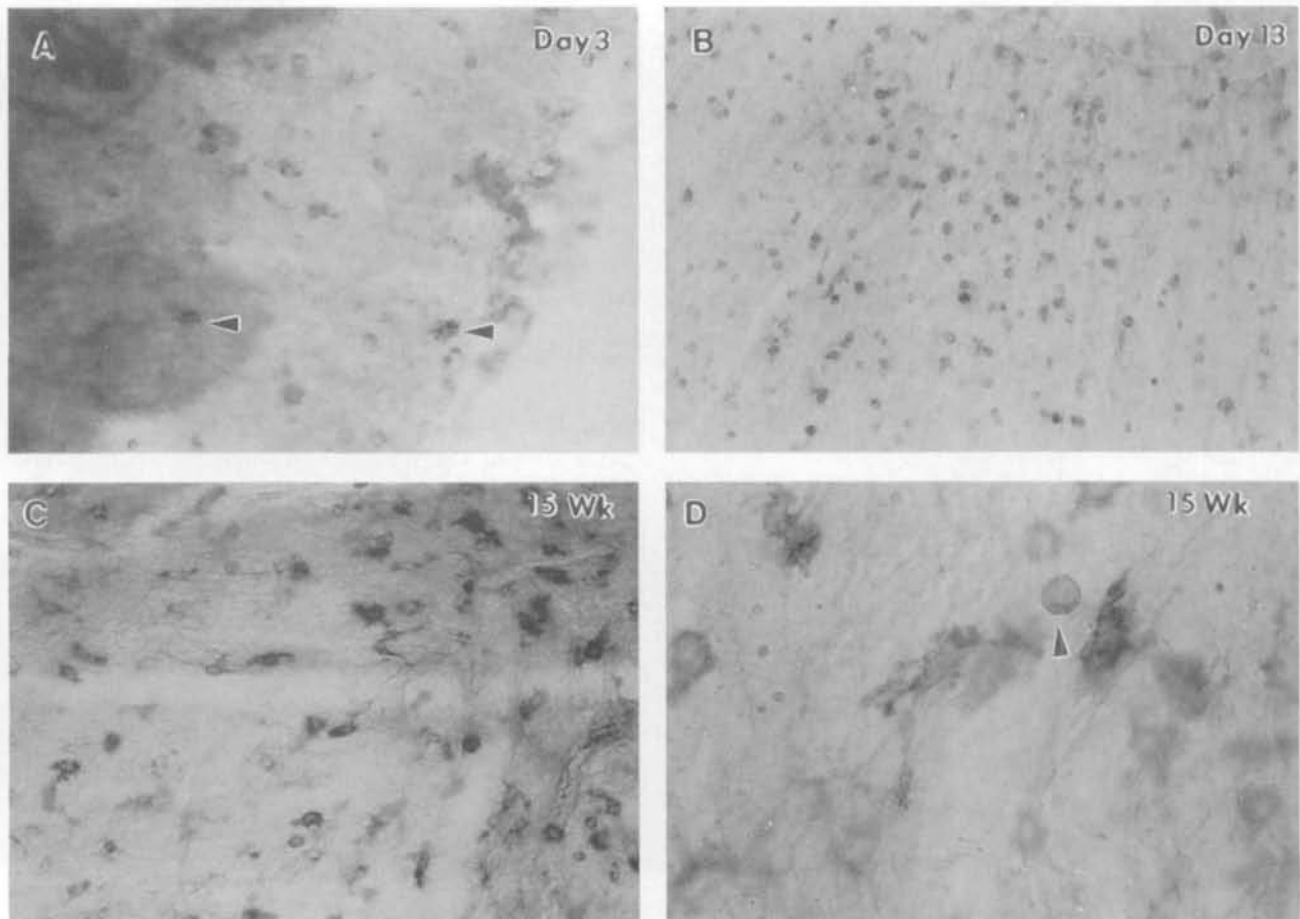


**FIGURE 7.** Coexpression of Ia antigens on OX62<sup>+</sup> iris dendritic cells. Ia was visualized with naphthol-AS-MX-phosphate and appears blue, the OX62 monoclonal antibody was visualized with aminoethylcarbazole and appears red, and cells coexpressing both antigens appear purple. (A) A 2- to 3-day-old animal: Immunopositive cells present in low numbers are predominantly OX62<sup>+</sup>/Ia<sup>-</sup> (red). OX62<sup>+</sup>/Ia<sup>+</sup> cells indicated by arrows. (B) A 13-day-old animal: OX62<sup>+</sup> cells are present at close to adult-equivalent levels; however, Ia coexpression and dendriform morphology are not well developed. (C) A 15-week-old animal: The major proportion of OX62<sup>+</sup> cells coexpress Ia and exhibit highly dendriform morphology. (D) High-power view of marginated OX62<sup>+</sup>/Ia<sup>-</sup> cell (arrow) in a 15-week-old animal. Magnifications: (A)  $\times 250$ , (B)  $\times 160$ , (C)  $\times 250$ , (D)  $\times 630$ . Original plate was in color, but cost prohibited publication.

development.<sup>12,35</sup> Findings in further immunostaining studies revealed that appearance of OX62<sup>+</sup> cells preceded that of Ia<sup>+</sup> DCs in the iris. Furthermore, the pattern of morphologic development and temporal increase in Ia coexpression suggested that Ia<sup>+</sup> DCs developed from the population of OX62<sup>+</sup>/Ia<sup>-</sup> cells. Knowing that virtually all Ia immunostaining within the iris was restricted to OX62<sup>+</sup> cells and the antigen recognized by the OX62 mAb is not expressed on monocytes,<sup>20</sup> it was concluded that OX62 expression within the iris was restricted to cells of the DC lineage and that the OX62<sup>+</sup>/Ia<sup>-</sup> cells observed comprised precursors of Ia<sup>+</sup> DCs. Such a finding is consistent with those in previous studies from this laboratory in which examination of the population kinetics of iris antigen-

presenting cell (APC) populations in adult eyes suggested a role for OX62<sup>+</sup>/Ia<sup>-</sup> cells as precursors of Ia<sup>+</sup> iris DCs.<sup>36</sup>

The results of the current study therefore indicate the ontogenic sequence of iris DC development. During late fetal development or around the time of birth, the developing iris is infiltrated through the vasculature by small, round (10 to 12  $\mu\text{m}$  in diameter) monocyte-like OX62<sup>+</sup>/Ia<sup>-/low</sup> cells that become distributed throughout the iris stroma. Influx of these OX62<sup>+</sup>/Ia<sup>-/low</sup> cells proceeds at a rate that establishes an adult-equivalent network of OX62<sup>+</sup> cells by postnatal day 13. During this period, OX62<sup>+</sup> cells grow larger, and a small proportion begin to express low to moderate levels of Ia. Whereas the OX62<sup>+</sup> cell population re-

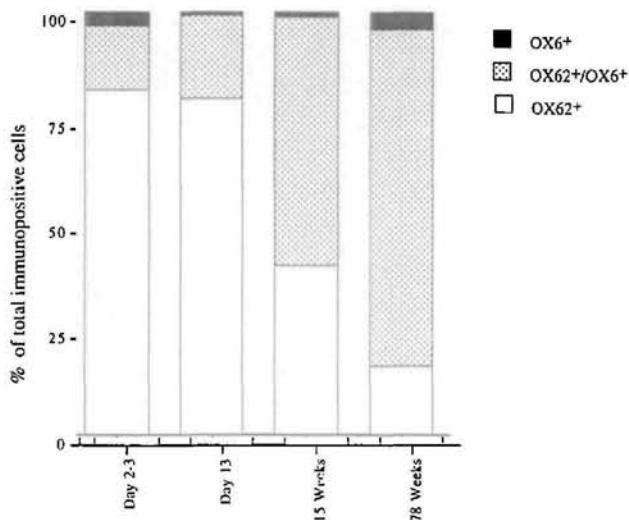


**FIGURE 8.** Quantitative assessment of Ia coexpression by OX62<sup>+</sup> iris dendritic cells during postnatal development. Data are compiled from three (15-week-old) or four (other age groups) animals per group.

mains relatively static after postnatal day 13, the development of Ia<sup>+</sup> DCs, as indicated by population density, level of Ia expression, and degree of dendriform structure, proceeds by transformation of this OX62<sup>+</sup>-Ia<sup>-/low</sup> population into OX62<sup>+</sup>-Ia<sup>+</sup> classic DCs. The presence of a residual population of small monocyte-like OX62<sup>+</sup>-Ia<sup>-/low</sup> cells in adult animals suggests that the relative static nature of the adult iris DC population may be maintained by continuous recruitment of these cells.

The precise nature of the circulating DC precursor cell that migrates into peripheral tissues is presently unclear, but it has been widely concluded that the small, round cells present in the early stages of DC population development represent such an infiltrating precursor.<sup>7,10,37,38</sup> Further evidence is provided by results of recent studies *in vitro*, which have established that the antigen recognized by the mAb OX62 is expressed on early Ia<sup>-</sup> predecessors of Ia<sup>+</sup> DCs propagated from rat bone marrow.<sup>34</sup> The ability of these propagated DCs to act as APC was reported to be acquired in parallel with Ia expression.<sup>34</sup> The fuzzy or spiked structure of the larger (12 to 15  $\mu$ m in diameter), rounded OX62<sup>+</sup>-Ia<sup>+</sup> cells observed in the iris was remarkably similar to that noted in DCs generated *in vitro* from CD34<sup>+</sup> human hematopoietic progenitor cells,<sup>39</sup> and low, buoyant density *in vitro* propagated DCs that had not fully matured.<sup>34</sup>

The mechanisms that induce DC maturation in nonlymphoid tissues are unclear. Some investigators suggest that exposure to environmental antigenic stimulation may provide the impetus for DC development.<sup>10,37,38</sup> However, it appears likely that although exogenous antigenic stimulation may accelerate the

process, it is not essential for DC development.<sup>11</sup> It is noted that the rate of development of Ia<sup>+</sup> iris DCs is greatest between postnatal days 13 and 21. This period coincides with eye opening, which in the rat occurs at approximately postnatal day 14. Eye opening is a major event in the development of ocular function and may impinge on the intraocular environment in many ways: through alteration of the regulation of components of the photodetection cascades, alteration in neuropeptide levels, or exposure of the globe to the external environment as a potential source of exogenous antigenic stimulation.

Morphogenesis of the rat iris commences late in gestation,<sup>40</sup> and at birth, it is represented by a narrow primordium. The presence of small, round Ia<sup>low</sup> cells within the iris primordium at 2 to 3 days after birth in the current study demonstrated that development of Ia<sup>+</sup> cells in this tissue commences close to the onset of iris morphogenesis. Despite the apparently rapid commencement of Ia<sup>+</sup> cell development in the iris, this population did not attain adult-equivalent characteristics and density until approximately 10 weeks of age. This contrasts distinctly with the development of those characteristics reported in many other nonlymphoid tissue sites of the rat—for example, the respiratory and gastrointestinal systems, where development of adult-density DC networks is generally complete by approximately 3 weeks after birth.<sup>5,6,8,10-13</sup> The mechanism underlying the temporal retardation of Ia expression by iris DCs compared with those in other tissue sites is unclear. One explanation is the postpartum development of the rat eye and anterior segment structures, in particular the iris, which persists until 6 months of age.<sup>41</sup> Alternatively, it is possible that the intraocular microenvironment within the AC exerts a modulatory influence on development of Ia expression. Tissues bordering the anterior chamber are bathed in aqueous humor, which contains high concentrations of transforming growth factor- $\beta$  (TGF- $\beta$ ).<sup>42</sup> Among the myriad of effects of this cytokine, is the capacity to antagonize interferon- $\gamma$ -induced upregulation of Ia and reduction of constitutive Ia expression in a range of cell types, including macrophages, microglia, and epithelia.<sup>43-45</sup> In addition to TGF- $\beta$ , aqueous humor contains high concentrations of free glucocorticoids<sup>46</sup> and vasoactive intestinal polypeptide,<sup>47</sup> both of which are capable of limiting MHC class II expression<sup>48-51</sup> and may delay the development of Ia expression by iris DCs.

It is feasible that OX62<sup>+</sup>-Ia<sup>-</sup> cells selectively accumulate within the iris vessels as a margined pool of cells, or within the iris tissue itself, where their further development is delayed or inhibited by the intraocular microenvironment. Whether OX62<sup>+</sup>-Ia<sup>-</sup> cells serve only as a pool of DC precursors or possess a unique functional significance is at present unclear and war-



rants further investigation. The results of the current study have provided a detailed account of the development of Ia<sup>+</sup> DCs in the iris of the rat and have extended the observations of McMenamin and Holt-house.<sup>14</sup> In doing so, the current findings have provided in vivo evidence of an OX62<sup>+</sup>-Ia<sup>-</sup> cell that is the likely proximate precursor of Ia<sup>+</sup> DCs in the iris, and possibly in other tissues. The results also demonstrate that rat iris DCs exhibit a pattern of development of Ia expression that is delayed compared with development in other tissue sites, suggesting the environment within the AC may exert a unique regulatory influence over iris DCs.

### Key Words

dendritic cell, eye development, iris, maturation, ontogeny,

### References

1. Knisely TL, Anderson TM, Sherwood ME, Flotte TJ, Albert DM, Granstein RD. Morphologic and ultrastructural examination of I-A<sup>+</sup> cells in the murine iris. *Invest Ophthalmol Vis Sci.* 1991;32:2423–2431.
2. McMenamin PG, Holthouse I, Holt PG. Class-II major histocompatibility complex (Ia) antigen-bearing dendritic cells within the iris and ciliary body of the rat eye—distribution, phenotype and relation to retinal microglia. *Immunology.* 1992;77:385–393.
3. McMenamin PG, Crewe J, Morrison S, Holt PG. Immunomorphologic studies of macrophages and MHC class II-positive dendritic cells in the iris and ciliary body of the rat, mouse, and human eye. *Invest Ophthalmol Vis Sci.* 1994;35:3234–3250.
4. Steptoe RJ, Holt PG, McMenamin PG. Functional studies of major histocompatibility class II-positive dendritic cells and resident tissue macrophages isolated from the rat iris. *Immunology.* 1995;85:630–637.
5. Wilders MM, Sminia T, Janse EM. Ontogeny of non-lymphoid and lymphoid cells in the rat gut with special reference to large mononuclear Ia-positive dendritic cells. *Immunology.* 1983;50:303–314.
6. van Rees EP, Dijkstra CD, van der Ende MB, Janse EM, Sminia T. The ontogenic development of macrophage subpopulations and Ia-positive non-lymphoid cells in gut-associated lymphoid tissues of the rat. *Immunology.* 1988;63:79–85.
7. Hsiao L, Takahashi K, Takeya M, Arao T. Differentiation and maturation of macrophages into interdigitating cells and their multicellular complex formation in the fetal and postnatal rat thymus. *Thymus.* 1991;17:219–35.
8. McCarthy KM, Gong JL, Telford JR, Schneeberger EE. Ontogeny of Ia<sup>+</sup> accessory cells in fetal and newborn rat lung. *Am J Respir Cell Mol Biol.* 1992;6:349–356.
9. Vicente A, Varas A, Alonso L, Demoral MG, Zapata AG. Ontogeny of rat thymic dendritic cells. *Immunology.* 1994;82:75–81.
10. Nelson DJ, McMenamin C, McWilliam AS, Brenan M, Holt PG. Development of the airway intraepithelial dendritic cell network in the rat from class II major histocompatibility (Ia)-negative precursors—differential regulation of Ia expression at different levels of the respiratory tract. *J Exp Med.* 1994;179:203–212.
11. Mayrhofer G, Pugh CW, Barclay AN. The distribution, ontogeny and origin in the rat of Ia-positive cells with dendritic morphology and of Ia antigen in epithelia, with special reference to the intestine. *Eur J Immunol.* 1983;13:112–122.
12. Darden AG, Forbes RD, Darden PM, Guttmann RD. The effects of genetics and age on expression of MHC class II and CD4 antigens on rat cardiac interstitial dendritic cells. *Cell Immunol.* 1990;126:322–30.
13. Fujiya H, Danilovs J, Brown J, Mullen Y. Species differences in dendritic cell distribution in pancreas during fetal development. *Transplant Proc.* 1985;17:414–416.
14. McMenamin PG, Holthouse I. Immunohistochemical characterisation of dendritic cells and macrophages in the aqueous outflow pathways of the rat eye. *Exp Eye Res.* 1992;55:315–324.
15. McMaster WR, Williams AF. Identification of Ia glycoproteins in the rat thymus and purification from the rat spleen. *Eur J Immunol.* 1979;9:426–433.
16. Brideau RJ, Carter PB, McMaster R, Mason DW, Williams AF. Two subsets of rat T lymphocytes defined with monoclonal antibodies. *Eur J Immunol.* 1980;10:609–615.
17. Dallman MJ, Mason DW, Webb M. The roles of host and donor cells in the rejection of skin allografts by T cell-deprived rats injected with syngeneic T cells. *Eur J Immunol.* 1982;12:511–518.
18. Hsiung L, Barclay AN, Brandon MR, Sim E, Porter RR. Purification of human C3b inactivator by monoclonal-antibody affinity chromatography. *Biochem J.* 1982;203:293–298.
19. Spickett GP, Brandon MR, Mason DW, Williams AF, Woollett GR. MRC OX-22, a monoclonal antibody that labels a new subset of T lymphocytes and reacts with the high molecular weight form of the leukocyte-common antigen. *J Exp Med.* 1983;158:795–810.
20. Brenan M, Puklavec M. The MRC OX-62 antigen: A useful marker in the purification of rat veiled cells with the biochemical properties of an integrin. *J Exp Med.* 1992;175:1457–1465.
21. Dijkstra CD, Dopp EA, Joling P, Kraal G. The heterogeneity of mononuclear phagocytes in lymphoid organs: Distinct macrophage subpopulations in the rat recognised by monoclonal antibodies ED1, ED2 and ED3. *Immunology.* 1985;54:589–599.
22. Hunig T, Wallny H-J, Hartley JK, Lawetsky A, Tiefenthaler G. A monoclonal antibody to a constant determinant of the rat T cell antigen receptor that induces T cell activation. *J Exp Med.* 1989;169:73–86.
23. Kuhnlein P, Park J-H, Herrman T, Elbe A, Hunig T. Identification and characterisation of rat  $\gamma/\delta$  T lymphocytes in peripheral lymphoid organs, small intestine, and skin with a monoclonal antibody to a constant determinant of the  $\gamma/\delta$  T cell receptor. *J Immunol.* 1994;153:979–986.
24. Sekiya S, Gotoh S, Yamashita T, Watanabe T, Saitoh S, Sendo F. Selective depletion of rat neutrophils by

- in vivo administration of a monoclonal antibody. *J Leuk Biol.* 1989;46:96–102.
25. Nicolls MR, Aversa GG, Pearce NW, et al. Induction of long-term specific tolerance to allografts in rats by therapy with an anti-CD3-like monoclonal antibody. *Transplantation.* 1993;55:459–468.
  26. Kroese FGM, Opstelten D, Wubbena P, et al. Monoclonal antibodies to rat B lymphocyte (sub-) populations. *Adv Exp Med Biol.* 1985;186:81–89.
  27. Kroese FG, Wubbena AS, Opstelten D, et al. B lymphocyte differentiation in the rat: Production and characterization of monoclonal antibodies to B lineage-associated antigens. *Eur J Immunol.* 1987;17:921–928.
  28. McMenamin PG, Crewe J. Endotoxin induced uveitis: Kinetics and phenotype of the inflammatory cell infiltrate and the response of the resident tissue macrophage and dendritic cells in the iris and ciliary body. *Invest Ophthalmol Vis Sci.* 1995;36:1949–1959.
  29. Snedecor GW, Cochran WG. *Statistical Methods.* Ames: Iowa State University Press; 1980.
  30. Barker CF, Billingham RE. Immunologically privileged sites. *Adv Immunol.* 1977;25:1–54.
  31. Streilein JW, Wilbanks GA, Cousins SW. Immunoregulatory mechanisms of the eye. *J Neuroimmunol.* 1992;39:185–200.
  32. MacPherson GG, Jenkins CD, Stein MJ, Edwards C. Endotoxin-mediated dendritic cell release from the intestine—characterization of released dendritic cells and TNF dependence. *J Immunol.* 1995;154:1317–1322.
  33. Forrester JV, McMenamin PG, Hothouse I, Lumsden L, Liversidge J. Localisation and characterisation of major histocompatibility complex class II-positive cells in the posterior segment of the eye: Implications for the induction of autoimmune uveoretinitis. *Invest Ophthalmol Vis Sci.* 1994;35:64–77.
  34. Chen–Woan M, Delaney CP, Fournier V, et al. A new protocol for the propagation of dendritic cells from rat bone marrow using recombinant GM-CSF, and their quantification using the mAb OX-62. *J Immunol Methods.* 1995;178:157–171.
  35. Hsiao L, Takeya M, Arao T, Takahashi K. An immunohistochemical and immunoelectron microscopic study of the ontogeny of rat Langerhans cells with anti-macrophage and anti-Ia antibodies. *J Invest Dermatol.* 1989;93:780–786.
  36. Steptoe RJ, Holt PG, McMenamin PG. Origin and steady-state turnover of major histocompatibility complex class II-positive dendritic cells and resident-tissue macrophages in the iris of the rat eye. *J Neuroimmunol.* 1996;68:67–76.
  37. Romani N, Schuler G, Fritsch P. Ontogeny of Ia-positive and Thy-1-positive leukocytes of murine epidermis. *J Invest Dermatol.* 1986;86:129–133.
  38. Elbe A, Tschachler E, Steiner G, Binder A, Wolff K, Stingl G. Maturation steps of bone marrow-derived murine epidermal cells. Phenotypic and functional studies on Langerhans cells and Thy-1<sup>+</sup> dendritic epidermal cells in the perinatal period. *J Immunol.* 1989;143:2431–2438.
  39. Caux C, Dezutter–Dambuyant C, Schmitt D, Banchereau J. GM-CSF and TNF-alpha cooperate in the generation of dendritic Langerhans cells. *Nature.* 1992;360:258–261.
  40. Reme C, Urner U, Aeberhard B. The development of the chamber angle in the rat eye. Morphological characteristics of developmental stages. *Graefes Arch Clin Exp Ophthalmol.* 1983;220:139–153.
  41. Reme C, Urner U, Aeberhard B. The occurrence of cell death during remodeling of the chamber angle in the developing rat eye. *Graefes Arch Clin Exp Ophthalmol.* 1983;221:113–121.
  42. Cousins SW, McCabe MM, Danielpour D, Streilein JW. Identification of transforming growth factor-beta as an immunosuppressive factor in aqueous humor. *Invest Ophthalmol Vis Sci.* 1991;32:2201–2211.
  43. Czarniecki CW, Chiu HH, Wong GHW, McCabe SM, Palladino MA. Transforming growth factor-beta modulates the expression of class II histocompatibility antigens on human cells. *J Immunol.* 1988;140:4217–4223.
  44. Suzumura A, Sawada M, Yamamoto H, Marunouchi T. Transforming growth factor-beta suppresses activation and proliferation of microglia in vitro. *J Immunol.* 1993;151:2150–2158.
  45. Donnet–Hughes A, Schiffrin EJ, Huggett AC. Expression of MHC antigens by intestinal epithelial cells. Effect of transforming growth factor-beta 2 (TGF-beta2). *Clin Exp Immunol.* 1995;99:240–244.
  46. Knisely TL, Hosoi J, Nazareno R, Granstein RD. The presence of biologically significant concentrations of glucocorticoids but little or no cortisol binding globulin within aqueous humour: Relevance to immune privilege in the anterior chamber of the eye. *Invest Ophthalmol Vis Sci.* 1994;35:3711–3723.
  47. Taylor, AW, Streilein JW, Cousins SW. Immunoreactive vasoactive intestinal peptide contributes to the immunosuppressive activity of normal aqueous humour. *J Immunol.* 1994;153:1080–1086.
  48. Snyder DS, Unanue ER. Corticosteroids inhibit murine macrophage Ia expression and interleukin 1 production. *J Immunol.* 1982;129:1803–1805.
  49. Warren MK, Vogel SN. Opposing effects of glucocorticoids on interferon-gamma-induced murine macrophage Fc receptor and Ia antigen expression. *J Immunol.* 1985;134:2462–2469.
  50. Frohman EM, Frohman TC, Vayuvegula B, Gupta S, van den Noort S. Vasoactive intestinal polypeptide inhibits the expression of the MHC class II antigens on astrocytes. *J Neurol Sci.* 1988;88:339–346.
  51. Celada A, McKercher S, Maki RA. Repression of major histocompatibility complex IA expression by glucocorticoids: The glucocorticoid receptor inhibits the DNA binding of the X box DNA binding protein. *J Exp Med.* 1993;177:691–698.